O3M SAF VSA ID O3_AS14_02

Evaluation of the possibility to derive reliable OClO slant columns from GOME2b and GOME2a spectra

Final report

Andreas Richter (IUP University of Bremen)

Folkard Wittrock (IUP University of Bremen)

Pieter Valks (German Aerospace Centre)

Status: Final 25.11.2015

Table of Contents

1 Introduction

1.1 Relevance of OClO in the atmosphere

In the stratosphere, the layer in the Earth's atmosphere extending from 8 to 50 km depending on latitude, a maximum is found in the ozone concentrations termed the ozone layer. Owing to its large absorption cross-section in the UV, this ozone efficiently filters most of the UV-A and UV-B contributions from the down-welling solar radiation. The ozone layer thereby provides an essential UV protection for life on the Earth's surface.

Ozone levels in the stratosphere are determined by an equilibrium of ozone production, which is driven by photolysis of oxygen, and ozone destruction, which is determined by photolysis of ozone and reaction with oxygen atoms (Chapman cycle). In addition, catalytic cycles including the NOx, BrOx and ClOx cycles reduce equilibrium levels of O_3.

Anthropogenic emissions of long-lived chlorine and bromine compounds which are transported into the stratosphere have increased stratospheric Bry and Cly loadings, offsetting the natural equilibrium. In particular in Polar Regions in spring, heterogeneous reactions of halogen reservoir substances on polar stratospheric clouds increase the concentrations of active halogen compounds to levels where a significant fraction of the total stratospheric ozone is removed (ozone hole). This results in increases in surface UV fluxes but also has important impacts on stratospheric dynamics.

Starting with the Montreal Protocol, a series of international treaties has successively banned ozone depleting substances, and atmospheric Cly and Bry levels have been reduced. Nevertheless, severe ozone depletion is still observed on a regular basis in polar spring, and it is expected that it will take until 2070 to return to pre-ozone hole levels of ozone.

In order to understand and track the development of stratospheric ozone, both ozone levels and the amounts of ozone depleting substances need to be monitored. In this context, UV-visible remote sensing observations can contribute with measurements of BrO and OClO in the stratosphere. The latter is formed by reaction of ClO and BrO and can thus provide indirect information on ClO levels.

1.2 Observations of OClO

Remote sensing measurements of OClO are performed by applying absorption spectroscopy in the 330 – 390 nm spectral region where the molecule exhibits characteristic absorption structures. As OClO photolyses rapidly, it can only be observed at large solar zenith angle, usually during twilight. Due to the sphericity of the Earth's atmosphere, the solar zenith angle changes along the light path from the sun to a point in the atmosphere, making the signal a complex mixture of the vertical OClO profile, its change with SZA and the light path. Therefore, OClO slant columns are usually not converted to vertical columns.

OClO columns have been retrieved using Differential Optical Absorption Spectroscopy (DOAS) measurements from the ground (Solomon et al., 1988, Kreher et al., 1996, Gil et al., 1996, Richter et al., 1999, Tørnkvist et al., 2002, Vandaele et al., 2005), from balloon (Renard et al., 1997), from aircraft (Schiller et al., 1990) and from satellite (Wagner et al., 2002, Richter et al., 2005, Krecl et al.,

2006, Fussen et al., 2006, Kühl et al., 2008). Nearly all OClO observations are focused on stratospheric applications and can detect OClO only when ClO is activated.

In spite of its very characteristic absorption features, the retrieval of OClO is difficult for several reasons. First of all, signals at low sun are small and therefore the signal to noise ratio is relatively poor. Second, depending on fitting window used, the ozone absorption can present a significant interference, and in addition has a large temperature dependence. Lastly, the ozone retrieval has proven to often have offsets, leading to positive or even negative columns in the absence of atmospheric OClO. These problems are present in all OClO retrievals. In GOME and SCIAMACHY data, lv1 calibration issues have shown to pose additional challenges.

With the launch of the first GOME2 instrument, it was expected that an OClO product could be developed in analogy to the GOME and SCIAMACHY OClO data. Using retrieval settings similar to those applied for SCIAMACHY, an OClO product could be developed for GOME2-A, which reproduces the overall pattern of chlorine activation. However, validation within an O3-SAF visiting scientist project (Richter et al., 2009) revealed a number of problems which were summarised as

- *There are many problems in the GOME-2 OClO data outside the regions of chlorine activation, leading to seasonal biases, sea-land contrast, cloud effects and scan angle dependencies. Some of the problems are known from other instruments (GOME-1, SCIAMACHY), pointing at retrieval issues. However, there also appears to be a lv1 data quality contribution.*
- *In comparison to SCIAMACHY (and GOME-1), the scatter of data is very large*.

Based on these results, the decision was taken not to make the GOME2-A OClO retrieval an operational product.

2 OClO retrieval on GOME2-B data

In October 2012, the second MetOp satellite was launched into orbit and since mid of December 2012, spectra from the GOME2-B instrument are available. The instruments on the two satellites are nearly identical, and it is expected that similar problems might arise in their lv1 and consequently also the lv2 products. However, calibration has shown that there are subtle differences which could affect the results. It also appears as if the GOME2-B lv1 data have better calibration than the GOME2-A spectra.

In this study, the possibility to derive an OClO product for GOME2-B is investigated. All retrievals were performed using the IUP-Bremen DOAS fitting software which is being used for data from many different DOAS instruments including the satellite instruments GOME, SCIAMACHY, GOME-2 and OMI. Systematic intercomparison with results obtained by retrieval codes from other groups (BIRA, MPI-Mainz, KNMI) has shown excellent agreement for both ground-based and satellite data. Previous transfers of IUP-Bremen DOAS products to operational SCIAMACHY and GOME-2 products have also shown that good agreement can be obtained between the operational products and the scientific data, and therefore it is expected, that the results found here are also valid for the operational processor.

2.1 Use of GOME2-A settings

As a first try, the settings developed for GOME2-A were applied to GOME2-B data (Fit A). The results were similar as those found for GOME2-B:

- OClO is successfully retrieved in conditions of chlorine activation
- The scatter of individual OClO retrievals is large
- There are large seasonal and latitudinal biases and a land-sea contrast
- There seems to be a drift in values over time

As an example, two selected days of data are shown in Figure 1.

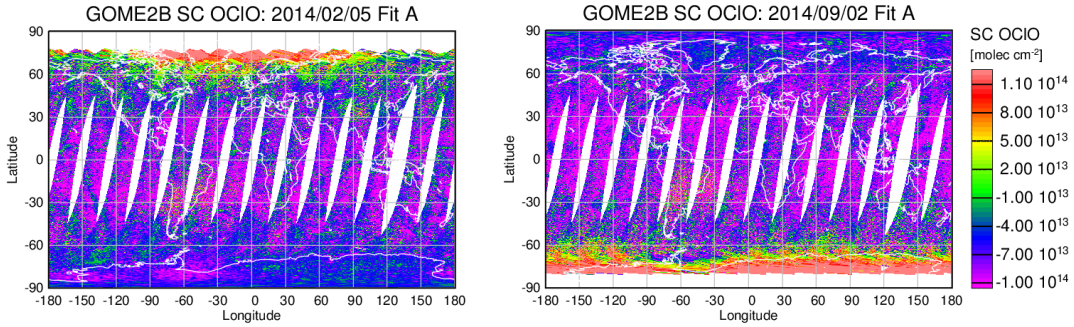

Figure 1: OClO slant columns from Fit A fro two example days.

2.2 Development of new settings

Starting from these results, three approaches were followed to improve the quality of the OClO products:

1. Use of a larger fitting window to reduce the noise
2. Inclusion of keydata to reduce the impact of calibration problems
3. Inclusion of empirical correction functions to reduce the impact of calibration problems

2.2.1 Large Fitting Window

In the literature, different fitting windows have been used for OClO retrieval having different advantages and disadvantages, mainly optimising either the signal or the degree of interference with ozone absorption structures. Here, the fitting window 345 - 389 nm was chosen which necessitates the inclusion of two absorption cross-sections of ozone taken at different temperature (Fit B).

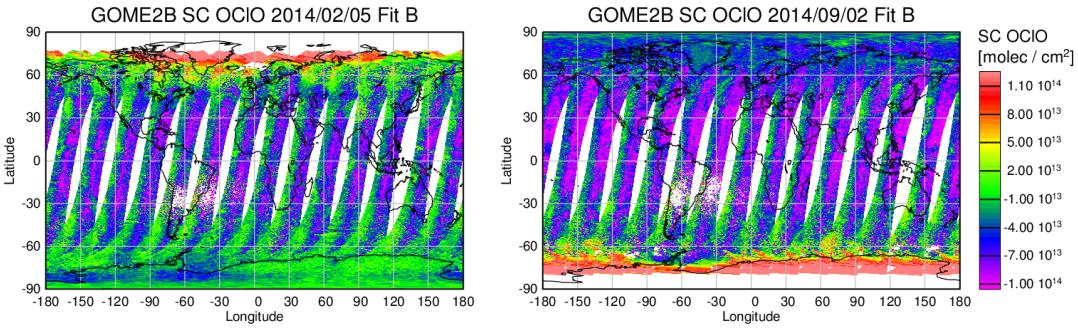

Figure 2: OClO slant columns from Fit B (large fitting window) for two example days.

As shown in Figure 2 for the two example days, the chlorine activation pattern is clearly reproduced in this retrieval and the scatter in data reduced as compared to Fit A. However, there is a pronounced scan angle dependence of the results and many negative values. This retrieval is thus not yet useful.

2.2.2 Inclusion of Eta

Experience with data from previous satellite instruments has shown that it sometimes is beneficial to include keydata obtained during calibration of the instrument as additional cross-sections in the fit to compensate for deficiencies in the lv1 calibration.

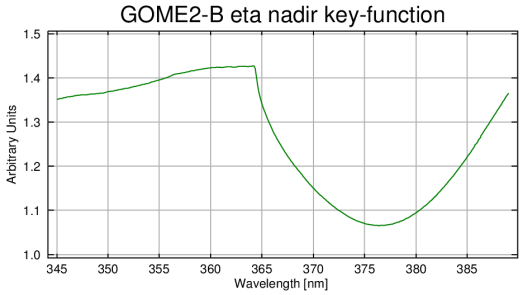

Figure 3: GOME2-B eta function in the OClO fitting range

Evaluation of fits including different keydata functions showed that using eta significantly improves the fitting residuals of the OClO fit in the large fitting window. This is to be expected as the polarisation correction of GOME2-B lv1 spectra is not perfect and the polarisation function eta has a clear spectral structure in the fitting region used (Figure 3).

As illustrated in Figure 4, the OClO slant columns increase substantially when including eta in the fit and less scan angle dependent structures are visible. However, the values are now biased high and there still remain systematically lower values in the eastern part of the scan.

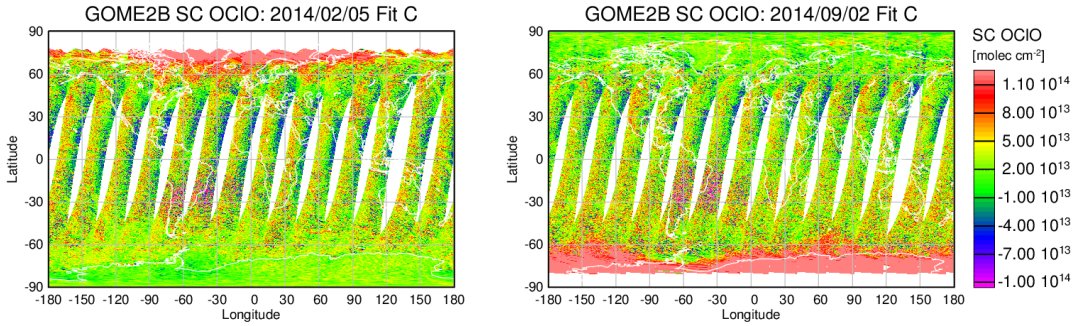

Figure 4: OClO slant columns from Fit C (large fitting window and eta) for two example days

2.2.3 Empirical corrections

Clearly, neither the large OClO columns over the tropical oceans, nor their scan angle dependence are realistic. In fact, no OClO is expected over this region. Therefore, a trick sometimes used in DOAS retrievals was investigated in which the mean residuals of a retrieval excluding OClO are introduced as additional (pseudo-) absorption cross-sections in the fit. More specifically, OClO was not included in the fit, and all spectra of GOME2-B from the arbitrarily selected day February 5, 2015 in the latitude range between 30°S and 30°N were fitted. The resulting residuals of the fits were divided

into three groups covering the viewing zenith angles of <- 30°, -30° - 30°, and >30°, respectively. From these three groups averages were formed and two spectra extracted, one for the central part of the scan representing the mean residual and one from the difference of the two outer groups representing the scan angle dependence of the residual.

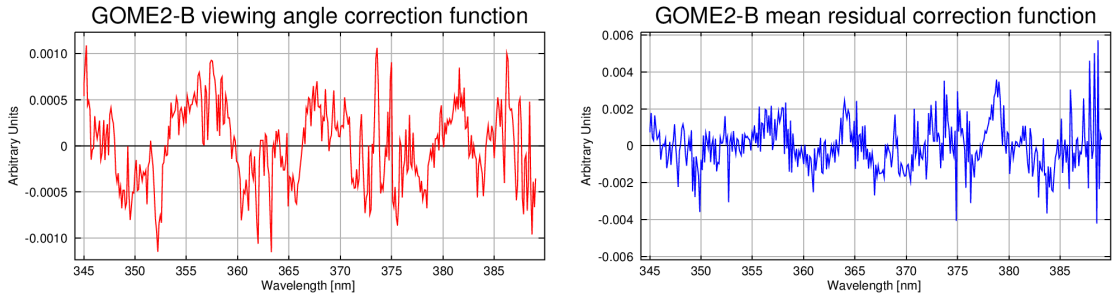

Figure 5: Empirical correction functions derived from the residuals from one day of fits excluding OClO and averaged between 30°S and 30°N. Left, the difference between the most eastern and most western parts of the residuals is shown; right the mean of the residuals in the centre part of the scan.

As can be seen in Figure 5, both cross-sections have high frequency and low frequency contributions and also show some similarities. These mean residuals contain a mixture of everything missing in the retrievals over the region selected: calibration problems, differences between the solar irradiance and earth-shine spectra, for example from slit function changes, inaccuracies in the absorption cross-sections used, including their convolution and also some noise.

When these two additional cross-sections are introduced in the fit, the results are significantly improved.

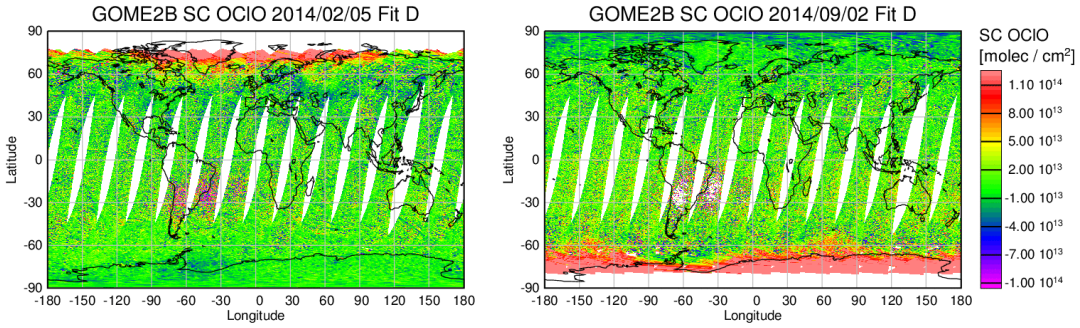

Figure 6: OClO slant columns from Fit D (large fitting window with eta and empirical functions) for two example days.

As illustrated in Figure 6, both the overall bias and the scan angle dependence of the OClO columns is removed while the high columns observed in regions of chlorine activation remain and the scatter of values has not increased. It is interesting to note that the day chosen for the extraction of the correction functions (05.02.2015) was many months later than the days used for the figure, indicating that the structures found can be applied over longer period of time and do not need to be re-calculated each day. Based on this very encouraging result, the complete available time series of GOME2-B data was analysed and the results evaluated.

Table 1: Overview on the GOME2-B fit parameters used. The highlighted Fit D represents the best choice

	Fit A	Fit B	Fit C	Fit D
window	365 – 389 nm	345 – 389 nm	345 – 389 nm	345 – 389 nm
polynomial	5 coeffs	5 coeffs	5 coeffs	5 coeffs
OClO	Kromminga et al., 1999	Kromminga et al., 1999	Kromminga et al., 1999	Kromminga et al., 1999
NO_2	Gür et al., 2005	Gür et al., 2005	Gür et al., 2005	Gür et al., 2005
O_4	Hermanns et al, 1999	Hermanns et al, 1999	Hermanns et al, 1999	Hermanns et al, 1999
Ring	Vountas et al., 1998	Vountas et al., 1998	Vountas et al., 1998	Vountas et al., 1998
O_3	-	Gür et al., 2005, 223 K and 243 K	Gür et al., 2005, 223 K and 243 K	Gür et al., 2005, 223 K and 243 K
offset	constant	linear	linear	linear
key-data	zeta	-	eta	eta
empirical functions	-	-	-	2

3 Evaluation of new settings

3.1 Scatter of Values

One of the main problems of the OClO product developed for GOME2-A was the large scatter of values. In order to evaluate the scatter in the new GOME2-B data set, all retrievals from May 2014 over the equatorial Pacific (160°-220°E, 20°S-20°N) were collected and a histogram of the distribution of values created. This was then compared to the same histogram for SCIAMACHY OClO retrievals from May 2008 and also to data from one day of retrievals using original (Fit A) settings.

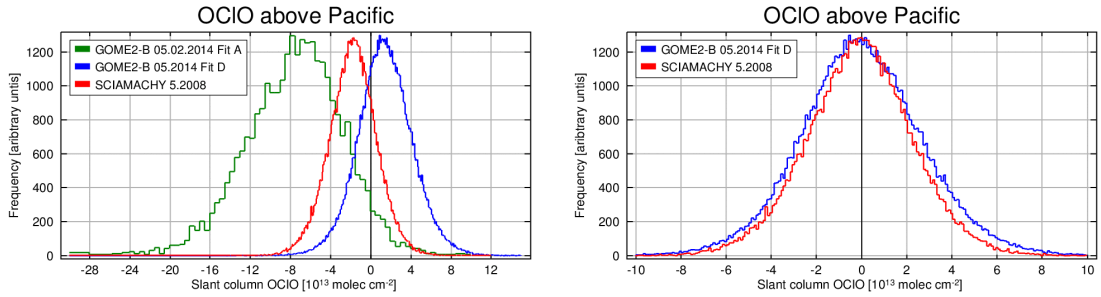

Figure 7: Histogram of OClO columns over the equatorial Pacific derived from GOME2-B data (blue: Fit D, Green: Fit A) and SCIAMACHY data (red). Histograms are scaled to have similar maximum. For GOME2-B, Fit A, only one day of data has been used and wider bins were applied.

As can be seen in Figure 7, the distribution of the new OClO columns over the equatorial Pacific is relatively close to 0 (mean bias around $1x10^{13}$ molec cm^{-2}) and has a similar width as the corresponding SCIAMACHY distribution. If both distributions are centred the comparison indicates that GOME2-B data still have a slightly larger spread with an FWHM of about $6x10^{13}$ molec cm^{-2}. Considering the fact that the exposure time for individual pixels is lower by a factor of 1.5 in GOME2, this is an excellent result.

3.2 Time evolution and offsets

One well known problem in OClO retrievals are offsets and temporal drifts in regions where no OClO is in the atmosphere. In order to characterize the behaviour of the GOME2-B OClO product in this

respect, data over the Pacific sector (180° - 220°E) were averaged in 10° latitude bins and their evolution plotted as a function of time. Ideally, all values should be close to 0 with the exception of high latitude regions during chlorine activation.

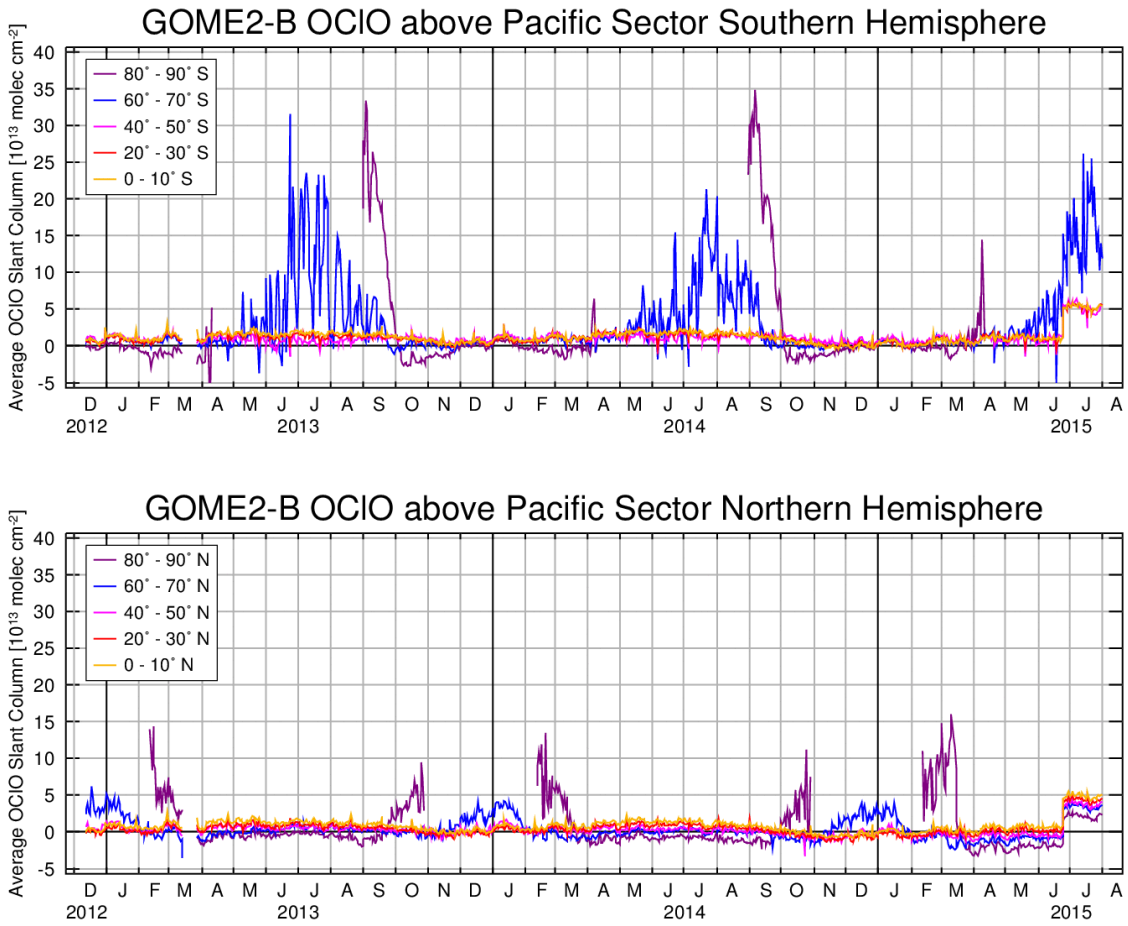

Figure 8: Time evolution of GOME2-B OClO columns (Fit D) for different latitude bands over the Pacific sector. Top: Southern hemisphere, bottom: Northern hemisphere.

As shown in Figure 8, GOME2-B OClO slant columns at latitudes < 50° have values always below $2x10^{13}$ molec cm^{-2} with a systematic seasonal variation showing a maximum in July / August. For the 60°-70° bins variability is much larger, in particular in the Southern Hemisphere due to irregular movements of the vortex bringing activated air masses in and out of the reference region. At higher latitudes, chlorine activation can be observed in both hemispheres, but also an increase in OClO in October in the NH which could be an artefact. Values at the highest latitude bin have a tendency for a low bias in times without chlorine activation. Overall, there appears to be a slight downward trend in NH values which is not clear in SH data.

After June 25, 2015, a sudden jump in offsets by about $5x10^{13}$ molec cm^{-2} is observed at all latitudes which is related to a change in lv1 processor version (Update to PPF 6.1) on June 26, 2015.

In summary, the offsets in the GOME2-B OClO data are systematic but small, certainly of the same order as in data from the GOME and SCIAMACHY instruments.

3.3 Sea-land contrast

One problem highlighted in previous GOME2-B OClO evaluations (Richter et al., 2009) but also for SCIAMACHY data is a clear sea-land contrast in regions where no OClO is expected. As shown in Figure 9, both positive and negative biases can be found over continents also in the new OClO product. However, there absolute size (up to $1.5x10^{13}$ molec cm^{-2} relative to the Pacific sector) is smaller and deemed to be acceptable in particular for studies having a focus on the Polar Regions,

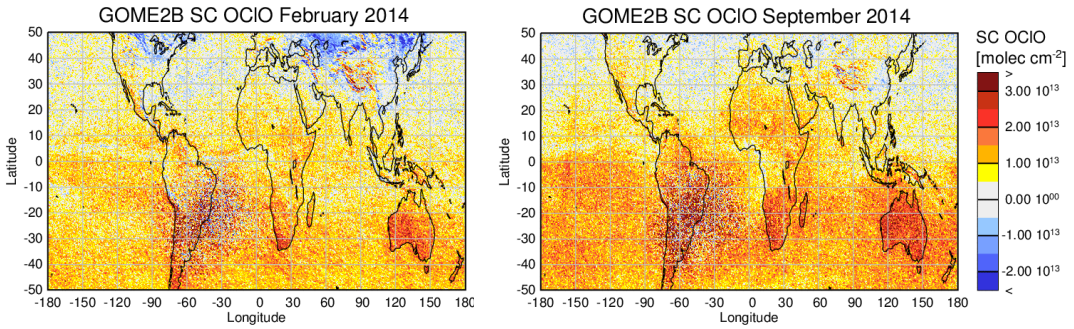

Figure 9: Zoomed-in view of GOME2-B OClO columns (Fit D) for February and September 20014. The colour scale has been chosen to highlight biases.

3.4 Scan angle dependence

As shown in section 2.2, there can be significant biases between OClO results from different parts of the scan. In particular the eastern part of the GOME2-B scan seems to have offsets relative to the other parts of the OClO retrievals.

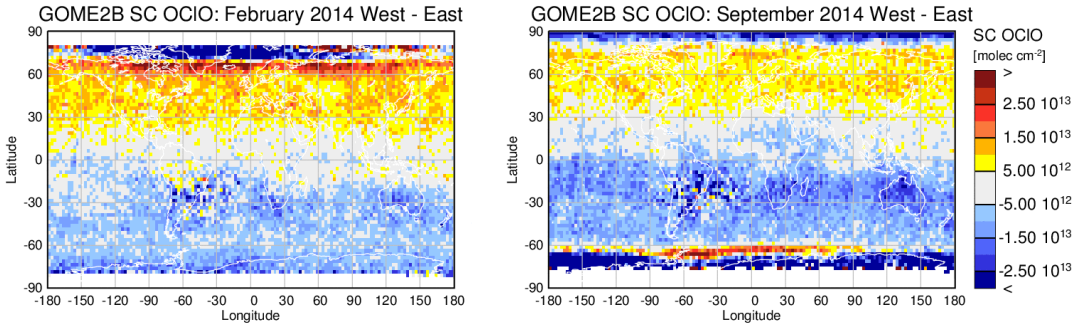

Figure 10: Differences in monthly averages of GOME2-B OClO slant columns (Fit D) when using only the western and the eastern part of the scan. Left: February 2014, right; September 2014. To reduce the noise, data have been binned on a 3.5° x 2.5° grid.

In Figure 10, differences are shown for monthly averages of GOME2-B OClO columns which were determined using only the eastern or western part of the scan, respectively. In regions of chlorine activation, larger values are expected for the Eastern part of the scan as solar zenith angles are systematically larger and thus OClO is less photolysed. This is reflected in the figures at high latitudes in the winter hemisphere. However, in regions without OClO, no difference is expected, and any signal is indicative of a retrieval bias. As can be seen from the figure, such biases exist, with higher west than east values in the NH and the opposite effect in the SH. However, the magnitude of the bias is mostly smaller than $1.5x10^{13}$ molec cm^{-2}, which for an OClO product is still acceptable.

4 Application of the GOME2-B OClO product

4.1 Monthly Averages

As individual OClO measurements are noisy, the data is best used with averaging. Different types of averaging can be performed – temporal averaging, spatial averaging around a location and spatial averaging over data in a range of solar zenith angles.

In Figure 12 and Figure 11, monthly averages of GOME2-B OClO slant columns are shown for the northern and southern hemisphere, respectively. The figures show the temporal evolution of the polar chlorine activation and the similarities and differences between years. As expected, OClO levels in the Southern hemisphere are larger and large values more widespread than in the Northern hemisphere. Differences between the years are larger in the Northern hemisphere with 2013 having lower chlorine activation levels and earlier de-activation than 2014 and 2015. In the Southern hemisphere, there are little differences between 2014 and 2015 observations. When focusing on the low OClO values outside the area of chlorine activation, a slight downward trend in the NH columns can be discerned, in agreement with Figure 8. Overall the values tend to be slightly negative. In the Southern hemisphere, values scatter around 0, changes are less obvious and if anything, a slight upward trend is present.

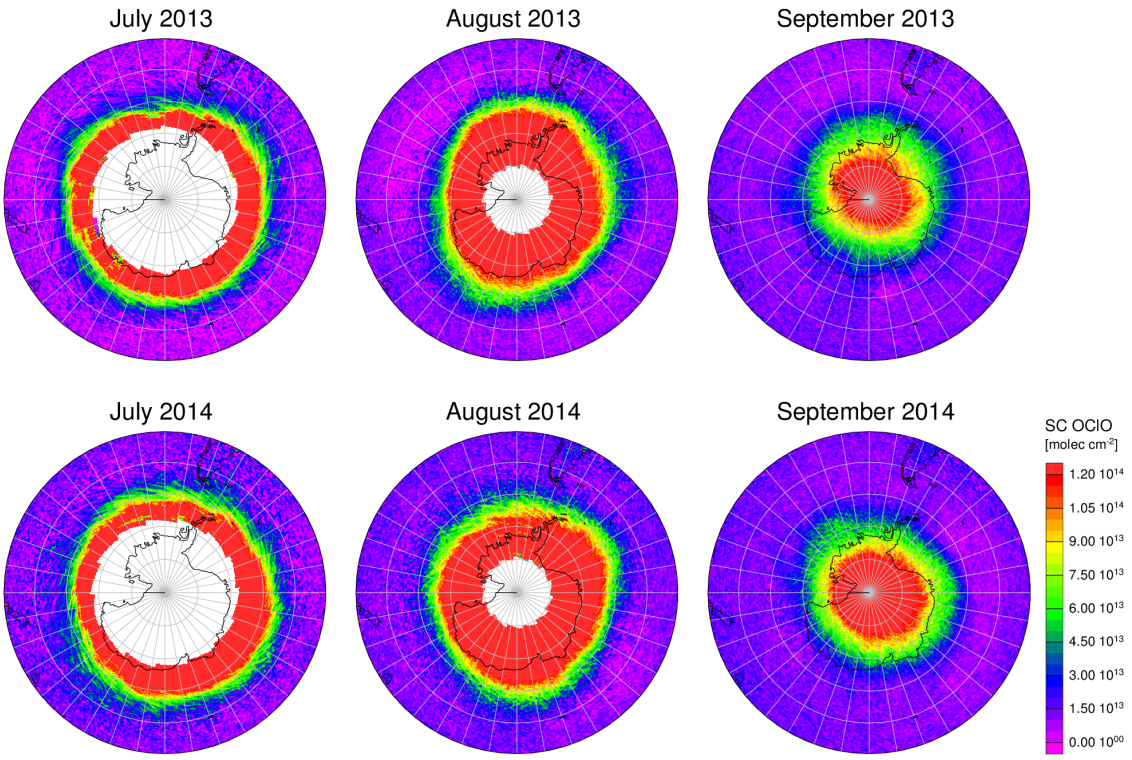

Figure 11: GOME2-B monthly means of OClO Slant Columns (Fit D) for the Southern hemisphere

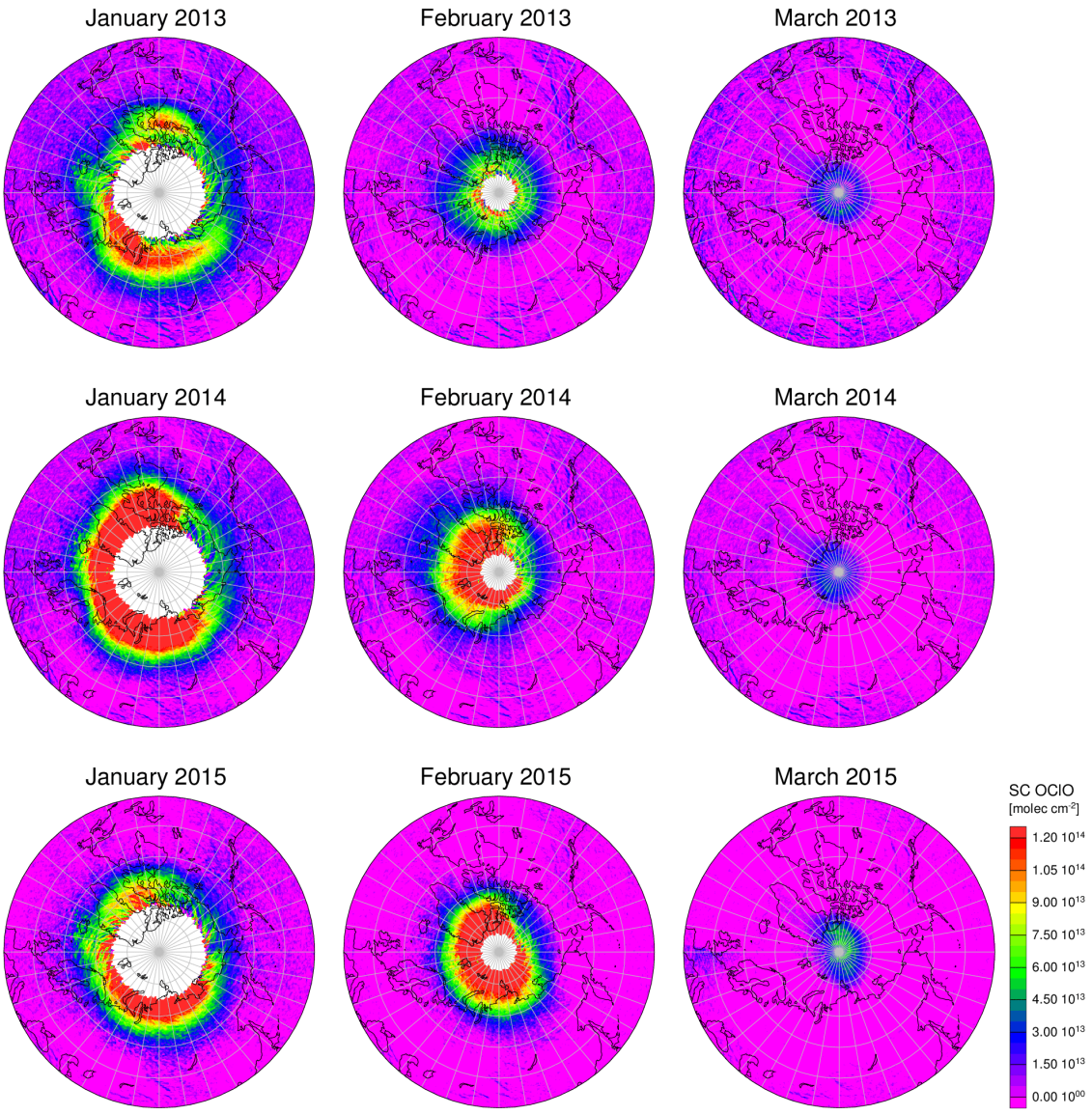

Figure 12: GOME2-B monthly means of OClO Slant Columns (Fit D) for the Northern hemisphere

4.2 Monitoring of Chlorine Activation

As the level of OClO columns depends critically on the solar zenith angle, a common way to present DOAS measurements of OClO is to extract values around 90°SZA and to create time series from these values. In satellite data, these averages cover a latitude band which changes over season, a complication which needs to be taken into account when interpreting the data. Here, all data having solar zenith angles in the range of 89 – 91° SZA have been averaged for each day of measurements separated by hemisphere. Only the descending parts of the orbits were considered.

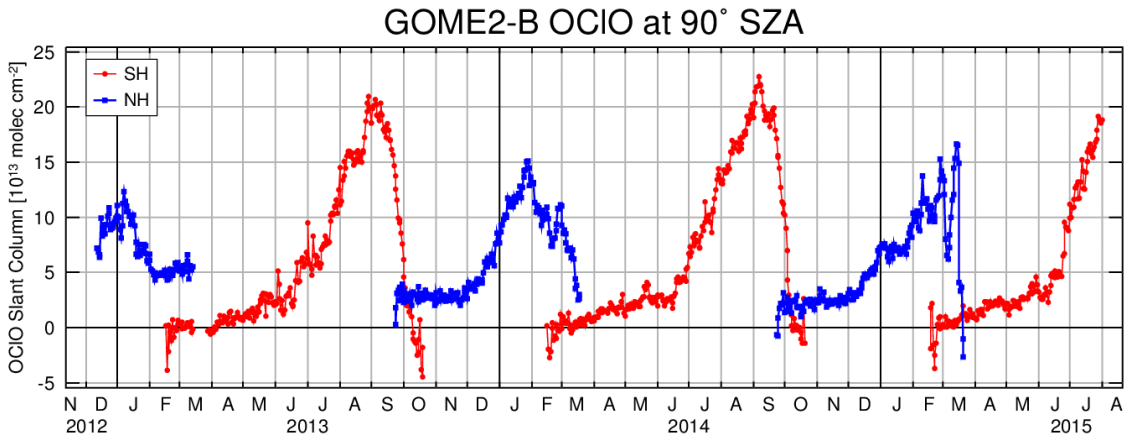

Figure 13: Daily GOME2-B OClO columns (Fit D) at 90° SZA for both hemispheres.

As shown in Figure 13, the daily 90° averages of GOME2-B OClO columns show little scatter with the exception of the start and end of the respective seasons where the number of measurement points decreases. Values before chlorine activation are very close to 0 in the Southern hemisphere and have a small offset of about 2×10^{13} molec cm^{-2} in the Northern hemisphere. The lower chlorine activation in 2013 can clearly be identified. After June 25, 2015, SH OClO columns appear larger than in previous years at the same time, in line with the offset discussed for Figure 8.

4.3 Validation with ground-based observations

In order to validate the GOME2-B OClO columns, a comparison was performed with ground-based zenith-sky observations in Ny-Ålesund (79°N, 12°E). Data from the ground-based DOAS instrument were analysed using an 80° SZA background spectrum from March 18 of the respective year. This is necessary as solar position at Ny-Ålesund changes rapidly in spring and 80° SZA is only reached in March at this latitude. Usually, ground-based data is interpreted by looking at 90° - 80° SZA differences in OClO slant column, assuming that at 80° SZA, most of the OClO is photolysed. For comparison with the satellite data, columns at the mean solar zenith angle of the satellite overpass were selected. This makes the two data sets comparable but is based on data at SZAs not usually evaluated, leading to increased scatter in the ground-based data.

The GOME2-B data were averaged over a 200 km radius around Ny-Ålesund to improve the signal to noise ratio. However, in particular at the onset of the measurements, the data are biased to the south of this averaging area as result of the latitude dependence of the solar zenith angle cut-off in the measurements. This is partly offset by using the mean solar zenith angle instead of the mean overpass time in the ground-based data.

By directly comparing the slant columns from ground-based and satellite observations, once makes the assumption that the light path is comparable. This is true in good approximation as discussed in Oetjen et al., 2011.

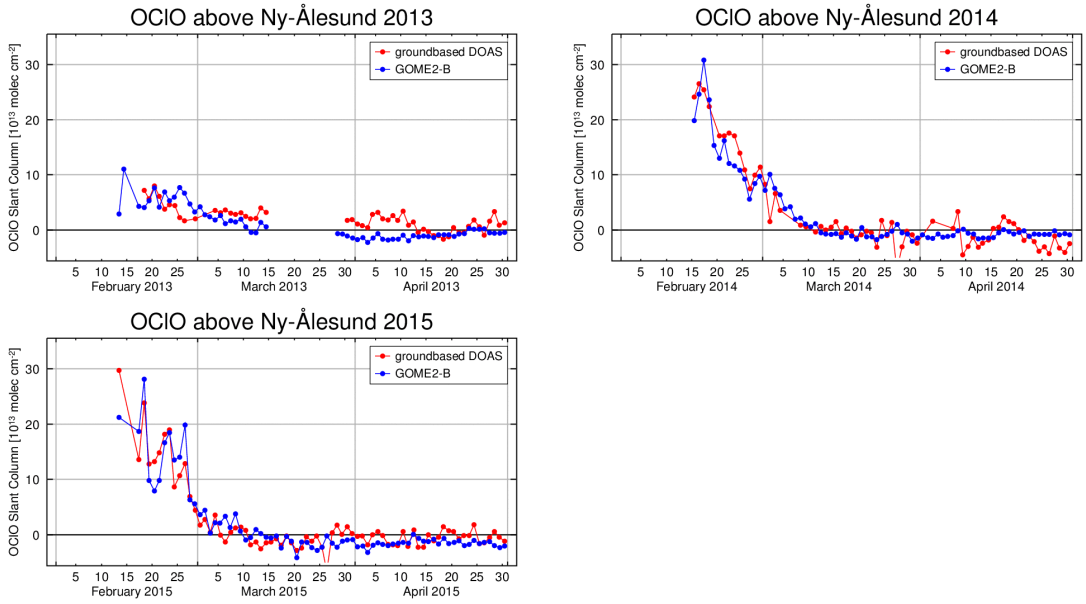

Figure 14: Comparison of ground-based and GOME2-B OClO slant columns over Ny-Ålesund. The ground-based measurements have been sampled at the time of satellite overpass. Satellite data have been averaged over a 200 km radius around the station to reduce the noise.

In Figure 14, the comparison between ground-based and GOME2-B OClO columns over Ny-Ålesund is shown for 2013, 2014, and 2015. Overall, the agreement is good with mean differences of the order of 1-2x10^{13} molec cm^{-2}. For individual points, differences can be larger, in part due to the significant scatter in the ground-based measurements, in particular in 2014 when there were some instrumental problems. However, the temporal evolution of the chlorine activation is in very good agreement, in particular considering the difference between 2013 and later years as well as the higher values in early March 2014 and the more variable columns in February 2015. The observed level of agreement is of the same order as that shown for SCIAMACHY data (Oetjen et al., 2011).

5 Application to GOME2-A data

With the good results obtained for GOME2-B using the revised retrieval settings, the same approach was applied to GOME2-A data in order to evaluate, whether or not OClO retrievals with sufficient accuracy are possible with these settings.

Table 2: Overview on the GOME2-A fit parameters used.

	Fit E
window	345 – 389 nm
polynomial	5 coeffs
OClO	Kromminga et al., 1999
NO_2	Gür et al., 2005
O_4	Hermanns et al, 1999
Ring	Vountas et al., 1998
O_3	Gür et al., 2005, 223 and 243 K
offset	linear
key-data	eta
empirical functions	1 (scan angle dependence)

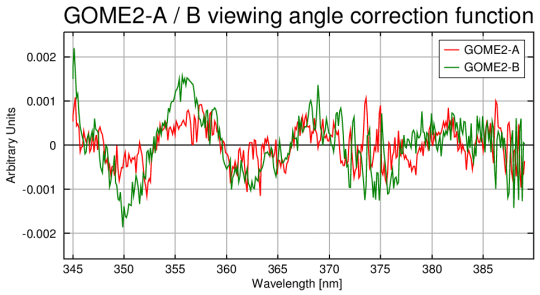

Figure 15: Scan angle dependency included in the OClO fit for GOME2-A (green) compared to the one derived for GOME2-A (red, same as in Figure 5 left)

First tests showed, that as for GOME2-B, the fit without empirical correction terms does not provide satisfactory results. Therefore, the same residual analysis as for GOME2-B was performed on data from August 29, 2008. Interestingly, the result for the scan angle dependency has a lot of similarity between the two instruments (see Figure 15) indicating similar origin of the problem, presumably optical degradation. Unlike for GOME2-B, it turned out that only the scan angle dependence needs to be taken into account while including the mean residual did not improve OClO columns. Therefore, the GOME2-A settings differ from the GOME2-B settings in that only one empirical correction term is included in the fit and that this is computed from GOME2-A data.

As for GOME2-B, GOME2-A OClO columns were evaluated over the Pacific sector for drifts and offsets. In Figure 16, the same type of analysis is shown as in Figure 8 for GOME2-B. There are some remarkable similarities and differences between these two sets of figures:

- Clearly, there is a downward trend in overall values in the first years of GOME2-A operation, most notable in the year after the second throughput test in September 2009. From 2011 onwards, data seems to be more stable.
- The seasonal variation for the low and mid-latitude bins is much larger than in GOME2-B data, in particular in the first years. The amplitude of this seasonality is strongly reduced after 2010. There are similar low biases at high latitudes as for GOME2-B, albeit with larger absolute values.
- As for GOME2-B, there is a jump in offsets after June 25, 2015.

The drifts noted in the sectors over the Pacific region are also found when applying the 90° SZA analysis from section 4.2 to the GOME2-A data. In 2007 – 2009, all values are high biased and after a transition in 2010, OClO columns in the SH appear to be low biased while little bias is apparent in NH data (Figure 17). In spite of these offsets, the data set nicely picks up the inter-annual variability in chlorine activation in the Northern hemisphere with low activation for example in 2008/2009 and the record activation in 2010/2011.

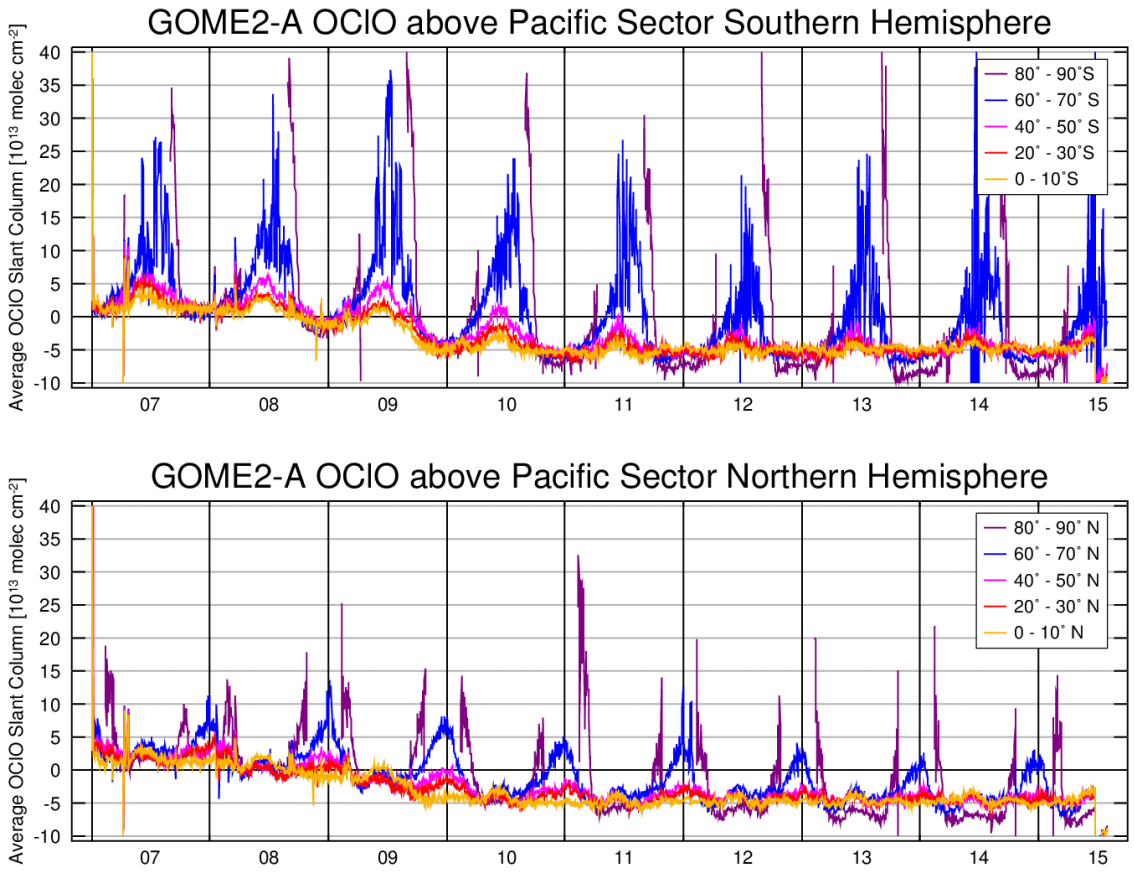

Figure 16: Time evolution of GOME2-A OClO columns for different latitude bands over the Pacific sector. Top: Southern hemisphere, bottom: Northern hemisphere.

In summary, the new GOME2-A OClO retrieval successfully picks up chlorine activation in both hemispheres at much lower noise than the original GOME2-A OClO evaluated in Richter et al., 2009. However, there are relatively large temporal drifts (> $5x10^{13}$ molec cm^{-2}) and changes in the seasonality of the slant columns at low and mid-latitudes which make additional correction necessary before the data can be applied for quantitative analysis.

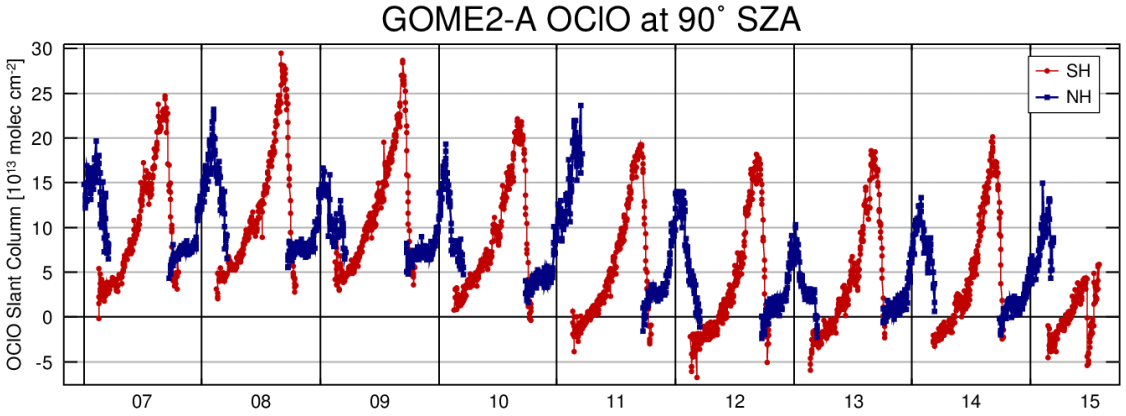

Figure 17: GOME2-A OClO columns at 90° SZA for both hemispheres.

5.1 Comparison of GOME2-A and GOME2-B data

In spite of the known issues in the GOME2-A OClO data, it is interesting to compare the results obtained from both instruments in the time period of overlapping measurements. This comparison is shown for the 90° time series as introduced in section 8 for both hemispheres.

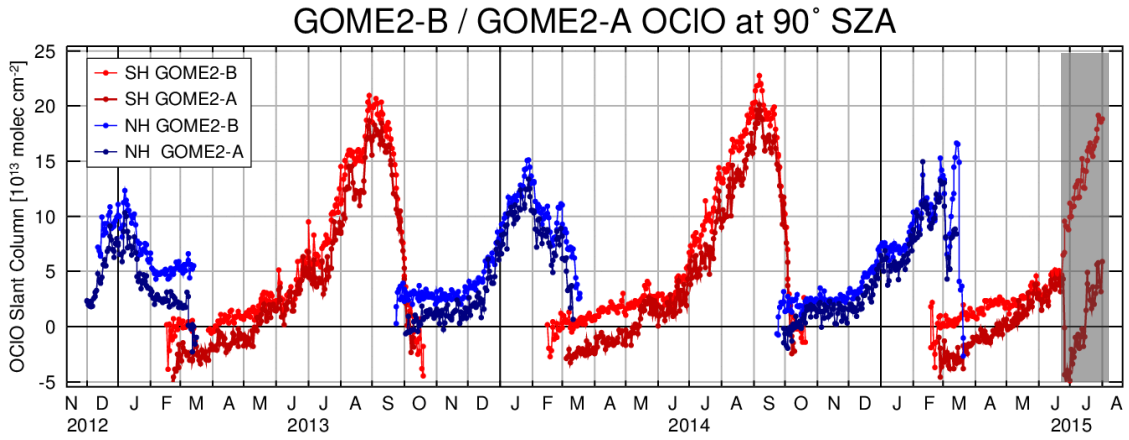

Figure 18: Comparison of GOME2-A and GOME2-B OClO at 90° SZA for both hemispheres. The shaded are marks the time after change in lv1 data version on June 26, 2015

As can be seen from Figure 18, both sensors yield very similar chlorine activation curves for the two hemispheres. There are, however, biases of the order of 1-2x10^{13} molec cm^{-2} between the two data sets, and these biases vary between hemispheres and over time. Judging from the measurements before chlorine activation starts, GOME2-A is less biased in the NH while GOME2-B looks better in the SH. In terms of absolute values, the agreement can still be considered as being good.

As mentioned previously, data after June 25 changed for both instruments, leading to large and opposing offsets which are larger than can be accepted.

6 Summary and Conclusions

In this study, the feasibility of a useful and reliable OClO slant column product from GOME2-A and GOME2-B spectra has been evaluated. To this end, sensitivity studies have been performed on measurements from both sensors, new retrieval parameters developed, the long-term evolution of the data sets has been evaluated, the results from the two sensors compared and finally the GOME2-B data set validated with ground-based zenith-sky observations.

The main conclusions for GOME2-B are

- Using a large fitting window, the eta keydata function and two empirical correction spectra, a satisfactory OClO product can be retrieved from the GOME2-B data
- The scatter of the GOME2-B product (FWHM of about 6x10^{13} molec cm^{-2}) is of comparable magnitude as for SCIAMACHY in spite of the larger number of measurements
- Chlorine activation in both hemispheres can be reliably detected in the GOME2-B data

- There are systematic biases which depend on latitude, season, sea-land and also viewing direction. The magnitude of the biases is relatively small (<2x10^{13} molec cm^{-2}) but changes over time. In particular after June 25, 2015, larger offsets are observed
- Validation with ground-based DOAS observations in Ny-Ålesund shows good agreement for the years 2013, 2014, and 2015

In summary, the GOME2-B OClO product is of similar quality as those for GOME and SCIAMACHY. It is useful for scientific applications in particular in Polar Regions and it is recommended to add it to the suite of operational products.

The main conclusions for GOME2-A are

- Using the large fitting window and an empirical correction spectrum, a reasonable OClO product can be derived from GOME2-A data, which has acceptable scatter and correctly detects chlorine activation in polar regions
- There are relatively large biases in the GOME2-A product which change over time
- The seasonality of the GOME2-A OClO product in regions where no OClO is expected is relatively large at the beginning of the mission and decreases over time. This could create problems in accurately detecting the onset of chlorine activation.
- The agreement of the GOME2-A OClO product at 90° SZA with the same quantity of GOME2-B is good with time varying offsets of 1-2x10^{13} molec cm^{-2}.

In summary, the OMGE2-A OClO product can be useful for scientific applications but only after offset correction. It is recommended to have at least a preliminary correction scheme in place before OClO becomes an operational GOME2-A product.

7 Outlook

Future work should mainly concentrate on compensation of offsets, in particular for GOME2-A and for the new data after June 25, 2015. The remaining problems with sea-land contrast and viewing dependencies are relatively small but further work is needed to better understand and possibly reduce them.

8 References

Fussen, D., Vanhellemont, F., Dodion, J., Bingen, C., Mateshvili, N., Daerden, F., Fonteyn, D., Errera, Q., Chabrillat, S., Kyrola, E., Tamminen, J., Sofieva, V., Hauchecorne, A., Dalaudier, F., Bertaux, J. L., Renard, J. B., Fraisse, R., d'Andon, O. F., Barrot, G., Guirlet, M., Mangin, A., Fehr, T., Snoeij, P., and Saavedra, L.: A global OClO stratospheric layer discovered in GOMOS stellar occultation measurements, *Geophys. Res. Lett.*, **33**, L13815, doi:10.1029/2006GL026406, 2006.

Gil, M., Puentedura, O., Yela, M., Parrondo, C., Jadhav, D. B., and Thorkelsson, B.: OClO, NO2 and O3 total column observations over Iceland during the winter 1993/94, *Geophys. Res. Lett.*, **23**, 3337–3340, 1996.

Gür, B., P. Spietz, J. Orphal and J. Burrows (2005), Absorption Spectra Measurements with the GOME-2 FMs using the IUP/IFE-UB´s Calibration Apparatus for Trace Gas Absorption Spectroscopy CATGAS, Final Report, IUP University of Bremen, Oct. 2005.

Hermans, C., Vandaele, A. C., Carleer, M., Fally, S., Colin, R., Jenouvrier, A., Coquart, B., and Merienne, M.-F.: Absorption cross-sections of atmospheric constituents: NO_2, O_2, and H_2O, *Environ. Sci. Pollut. R.* , **6**, 151–158, 1999.

Krecl, P., Haley, C. S., Stegman, J., Brohede, S. M., and Berthet, G.: Retrieving the vertical distribution of stratospheric OClO from Odin/OSIRIS limb-scattered sunlight measurements, *Atmos. Chem. Phys.*, **6**, 1879–1894, doi:10.5194/acp-6-1879-2006, 2006.

Kreher, K., Keys, J. G., Johnston, P. V., Platt, U., and Liu, X.: Ground-based measurements of OClO and HCl in austral spring 1993 at Arrival Heights, Antarctica, *Geophys. Res. Lett.*, **23**, 1545–1548, 1996.

Kromminga, H., Orphal, J., Spietz, P., Voigt, S., Burrows, J.P., New measurements of OClO absorption cross sections in the 325-435 nm and their temperature dependence between 213-293 K. *J. Photochem. Photobiol. A.*: Chemistry, **157**, 149-160, 2003.

Kühl, S., Pukite, J., Deutschmann, T., Platt, U., and Wagner, T.: SCIAMACHY limb measurements of NO2, BrO and OClO, Retrieval of vertical profiles: Algorithm, first results, sensitivity and comparison studies, *Adv. Space Res.*, **42**, 1747–1764, doi:10.1016/j.asr.2007.10.022, 2008.

Oetjen, H., Wittrock, F., Richter, A., Chipperfield, M. P., Medeke, T., Sheode, N., Sinnhuber, B.-M., Sinnhuber, M., and Burrows, J. P.: Evaluation of stratospheric chlorine chemistry for the Arctic spring 2005 using modelled and measured OClO column densities, *Atmos. Chem. Phys*., **11**, 689-703, doi:10.5194/acp-11-689-2011, 2011.

Renard, J. B., Lefevre, F., Pirre, M., Robert, C., and Huguenin, D.: Verticle profile of night-time stratospheric OClO, *J. Atmos. Chem.*, **26**, 65–76, 1997.

Richter, A., M. Eisinger, A. Ladstätter-Weißenmayer and J. P. Burrows, DOAS zenith sky observations. 2. Seasonal variation of BrO over Bremen (53°N) 1994-1995, *J. Atm. Chem.*, **32**, 83-99, 1999.

Richter, A., F. Wittrock, M. Weber, S. Beirle, S. Kühl, U. Platt, T. Wagner, W. Wilms-Grabe, and J. P. Burrows, GOME observations of stratospheric trace gas distributions during the splitting vortex event in the Antarctic winter 2002 Part I: Measurements, *J. Atmos. Sci.*, **62** (3), 778-785, 2005.

Richter A., Slijkhuis S., Loyola D., Offline Total OClO validation report, O3M-11, 2009. (http://www.iup.uni-bremen.de/doas/reports/o3saf_vs_gome-2_oclo_finalreport_091208.pdf)

Schiller, C., Wahner, A., Platt, U., Dorn, H. P., Callies, J., and Ehhalt, D. H.: Near UV atmospheric absorption measurements of column abundances during Airborne Arctic Stratospheric Expedition, January-February 1989: 2. OClO observations, *Geophys. Res. Lett.*, **17**, 501–504, 1990.

Solomon, S., Mount, G. H., Sanders, R. W., Jakoubek, R. O., and Schmeltekopf, A. L.: Observations of the nighttime abundance of OClO in the winter stratosphere above Thule, Greenland, *Science*, **242**, 550–555, 1988.

Tørnkvist, K. K., Arlander, D. W., and Sinnhuber, B. M.: Ground-based UV measurements of BrO and OClO over Ny-Ålesund during winter 1996 and 1997 and Andøya during winter 1998/1999, *J. Atmos. Chem.*, **43**, 75–106, 2002.

Vandaele, C., et al., An intercomparison campaign of ground-based UV-visible measurements of NO2, BrO, and OClO slant columns: Methods of analysis and results for NO2, *JGR*, **110**, doi:10.1029/2004JD005423, 2005.

Wagner, T., F. Wittrock, A. Richter, M. Wenig, J. P. Burrows, and U. Platt, Continuous monitoring of the high and persistent chlorine activation during the Arctic winter 1999/2000 by the GOME instrument on ERS-2, *J. Geophys. Res.*, doi:10.1029/2001JD000466, 2002.